ISSN 1063-7788, Physics of Atomic Nuclei, 2019, Vol. 82, No. 4, pp. 317–323. © Pleiades Publishing, Ltd., 2019.

NUCLEI
Theory

Triaxiality in Neutron-Rich As Isotopes with Covariant Density Functional Theory

T. Bayram[1),2)*]

Received February 24, 2019; revised March 15, 2019; accepted March 15, 2019

Abstract—The relativistic mean-field model with density-dependent DD-ME2 and DD-PC1 interactions has been used for the investigation of the ground-state shape evolution of neutron-rich $^{83-91}$As isotopes. For this purpose, the potential energy curve and the potential energy surface of each nucleus of interest have been examined. From analyzing the potential energy surfaces of the neutron-rich $^{83-91}$As isotopic chain, ^{87}As is suggested to be a possible candidate for triaxial nucleus. Furthermore, studies of some ground-state nuclear properties of As isotopes such as energy, size and deformation have been obtained.

DOI: 10.1134/S1063778819040045

1. INTRODUCTION

One of the hottest topic in the experimental and theoretical nuclear structure studies is nuclear shape evolution [1, 2]. Nuclei can exhibit geometrically spherical, axially deformed and γ-soft rotor shapes in their ground-state (g.s.). Some interesting phenomena such as shape coexistence, triaxiality, and shape phase transitions between these geometrical shapes can occur [3, 4]. As is well known, nuclei along the $N = Z$ region, starting from the Ni ($Z = 28$) to Sn ($Z = 50$), exhibit rapid shape changes and shape-coexistence phenomena. Starting from the low-Z values, the g.s. shape evolves from spherical for the double-magic ^{56}Ni, triaxial in ^{64}Ge, to oblate for ^{68}Se and ^{72}Kr [5–8]. Triaxial deformation of an atomic nucleus is related to wobbling motion and nuclear chirality [9]. From the experimental viewpoint, observing of chiral doublet and wobbling bands is used as to be a direct evidence for the triaxiality of nuclei. Around the $A = 100$ mass region, study of not only triaxial deformation but also triaxial shape transition along with the increasing neutron number has been attractive (see [9] and references therein). Besides, the experimental determinations of band structures of nuclei cannot be an easy task when the neutron-rich nuclei are considered. In such a case, reliable model predictions are favorable. More recently, structural evolution of germanium and selenium nuclei within the mapped interacting boson model based on the Gogny energy density functional has been studied in [10]. On the neutron-rich side around $N = 60$, γ-soft character of Ge and Se nuclei has been identified. Therefore, an investigation of the g.s. shape evolution of the neutron-rich As nuclei located between Ge and Se nuclei can be interesting.

For precise determining the g.s. shape of a nucleus, experimental observations are necessary such as some low-lying levels and the ratio of reduced electric quadrupole transitions which can be obtained from the life-time measurements. Such experimental data can be analyzed by means of predictions of algebraic models as prescribed in [4] for determining the g.s. shape of nuclei and the quantum phase transitions in nuclei. On the other hand, it cannot be easy to reach spectral data of nuclei when they are close to the neutron and proton drip-lines as in the case of neutron-rich As isotopes. Because the existence of triaxially deformed nuclei is an attractive topic, there can be found many studies where triaxiality in nuclear g.s. and at small angular momenta is suggested (see [11] and references therein). The corresponding minima in the energy surfaces are generally soft for triaxial nuclei.

The mean-filed formalism has been used in nuclear structure studies for more than four decades. Non-relativistic density functionals based on density-dependent forces, such as Skyrme [12] or Gogny [13] functionals, are successfully used for the investigation of the g.s. nuclear properties of nuclei. As its relativistic counterparts, the relativistic mean-field (RMF) theory which is also called as the covariant density fucntional theory after adding density dependence has also gained much attention for the investigation of the g.s. properties of nuclei at and far from stability [14–20]. It is also used for the investigation

[1)]Department of Physics, Karadeniz Technical University, 61080 Trabzon, Turkey.
[2)]INFN, Laboratori Nazionali di Legnaro, 35020 Legnaro (PD), Italy.
[*]E-mail: t.bayram@ktu.edu.tr

of the g.s. shape evolution of many isotopic chains of nuclei (see [21] and references therein). In many studies, the potential energy curve (PEC) and/or the potential energy surface (PES) obtained from the constrained RMF model calculations have been examined for the quantitative determination of the g.s. shape evolution of nuclei.

In the present paper, we have performed the RMF model calculations with two different density-dependent interactions for the investigation of the g.s. nuclear properties of neutron-rich $^{83-91}$As isotopes. The binding energy per nucleon (BE/A), two-neutron separation energy (S_{2n}), root-mean-square (rms) charge radii (r_c), quadrupole deformation parameter (β_2) and total quadrupole moment (Q_t) of the considered nuclei have been obtained. By using constrained RMF calculations, we have produced PEC and PES of $^{83-91}$As isotopes for the discussion its of g.s. shape evolution. As will be discussed later, ^{87}As nucleus is suggested to be a possible candidate for triaxial deformed nucleus quantitatively.

The paper is organized in the following way. The RMF model is summarized in Section 2, while details of calculations are given in Section 3. The results of the present study and discussion are given in Section 4 and, finally, in Section 5 conclusions are given.

2. THEORETICAL FRAMEWORK

In the RMF model, nucleons are introduced as Dirac particles and they interact with each other by the exchange of various mesons and photons [22]. Dirac particles move independently as relativistic particles in an average potential created by other nucleons. The mesons are taken into account for the description of the nuclear force between the nucleons properly in such a way that the scalar σ and vector ω mesons are responsible for the attractive and repulsive part of the interaction of nucleons, respectively. The isovector vector ρ meson and photon are for providing isospin-dependent effects and the electromagnetic interactions in nuclei, respectively. σ, ω and ρ mesons are commonly considered in the RMF model. In the first version of RMF model [22], the interactions of mesons among themselves were not considered. Later, it was understood that the model was not sufficient for the description of incompressibility and nuclear surface properties for nuclear matter. Therefore, Boguta and Bodmer [23] have added a non-linear self-interaction term of the σ mesons. In recent two decades, more reliable versions of the RMF model such as non-linear self-interaction of the ω and ρ mesons and density-dependent meson–nucleon coupling have been introduced for more precise predictions of the g.s. properties of finite nuclei [24–28]. Thus, RMF theory started to be called the covariant density functional theory because of its density dependence. In this section we summarize the basics of the RMF theory only by means of medium dependent vertices.

The interaction mechanism of the RMF model which includes terms for free nucleons, mesons and nucleon–meson interactions is represented with a phenomenological Lagrangian density $\mathcal{L}$ given by

$$\begin{aligned}\mathcal{L} = {} & \bar{\psi}(i\gamma\partial - m)\psi + \frac{1}{2}(\partial\sigma)^2 - \frac{1}{2}m_\sigma^2\sigma^2 - \frac{1}{4}\mathbf{\Omega}_{\mu\nu}\mathbf{\Omega}^{\mu\nu} \\ & + \frac{1}{2}m_\omega^2\omega^2 - \frac{1}{4}\mathbf{R}_{\mu\nu}\mathbf{R}^{\mu\nu} + \frac{1}{2}m_\rho^2\rho^2 \\ & - \frac{1}{4}\mathbf{F}_{\mu\nu}\mathbf{F}^{\mu\nu} - g_\sigma\bar{\psi}\sigma\psi - g_\omega\bar{\psi}\gamma\omega\psi \\ & - g_\sigma\bar{\psi}\gamma\rho\tau\psi - A\frac{1-\tau_3}{2}\psi, \end{aligned} \quad (1)$$

where the masses of mesons (fields) are represented with m_σ (σ), m_ω (ω), and m_ρ (ρ). The meson–nucleon couplings of the considered mesons are denoted by g_σ, g_ω and g_ρ, respectively. Dirac spinor for nucleons with mass (m) is represented by ψ. The bold-type symbols represent space vectors. In Eq. (1), the first term is related with free nucleons, while the latter four terms are related with meson–nucleon interactions. The rest terms are for free mesons. Field tensors given in Eq. (1) are given by

$$\begin{aligned}\mathbf{\Omega}^{\mu\nu} &= \partial^\mu\omega^\nu - \partial^\nu\omega^\mu, \\ \mathbf{R}^{\mu\nu} &= \partial^\mu\rho^\nu - \partial^\nu\rho^\mu, \\ \mathbf{F}^{\mu\nu} &= \partial^\mu A^\nu - \partial^\nu A^\mu. \end{aligned} \quad (2)$$

For parity transformation, the Lagrangian density is invariant and the expectation value of the pseudoscalar pion field vanishes in the mean-field approximation. Coupling constants and unknown meson masses are adjusted from the experimental data. Equations of motion as a couple of set of differential equations for the fields are obtained by performing the variational principle on the Lagrangian density given in Eq. (1) and these equations are called RMF equations. The RMF equations can be solved iteratively. The latest computer code for the solution of symmetric, axially deformed and triaxially deformed RMF equations can be found in [29].

3. DETAILS OF CALCULATIONS

In the present study, the g.s. properties of neutron-rich $^{83-91}$As isotopes, such as binding energy, charge radii, quadrupole moment and deformation parameter, have been calculated by using the RMF model with two functionals DD-ME2 [30] and DD-PC1 [31]. For these calculations the DIRHB code has been used [29]. Both axially deformed

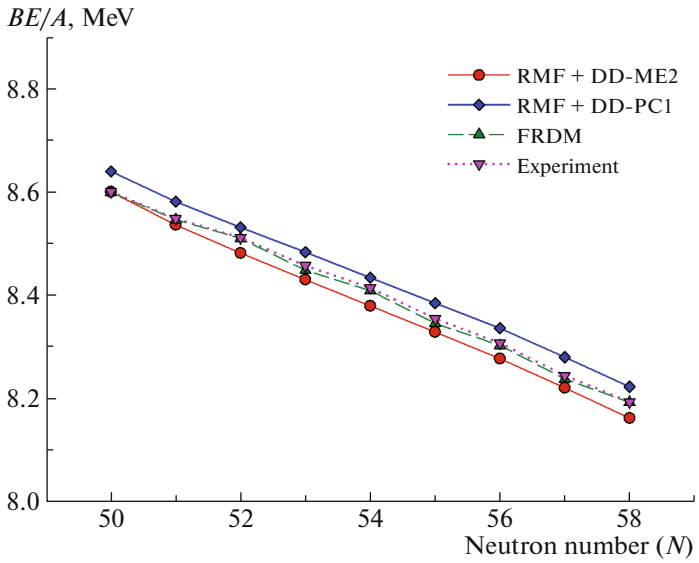


Fig. 1. The calculated BE/A of neutron-rich $^{83-91}$As isotopes with DD-ME2 and DD-PC1 interactions in comparison with those of FRDM and experimental data. See text for details.

and triaxially deformed symmetric cases within the framework of the RMF model have been taken into account for PEC and PES of each As nuclei. For obtaining PECs, the quadrupole moment constrained RMF model have been employed with fixed values of the electric quadrupole deformation parameter β_2 starting from the $\beta_2 = -0.5$ (oblate) to $\beta_2 = 0.5$ (prolate). In the axially symmetric RMF equation solutions, the constant gap approximation for pairing correlations has been taken into account as prescribed in [32]. The initial pairing gap has been taken to be $\Delta_p = 4.8/(Z)^{1/3}$ and $\Delta_n = 4.8/(N)^{1/3}$ for proton and neutron, respectively. The considered shell number was 12 and 20 for fermions and bosons, respectively. For obtaining the PESs of neutron-rich isotopic chain of As nuclei, the triaxially deformed RMF model calculations have been carried out. In this case, the BE of As nuclei of interest has been calculated by fixing β_2 ($0 \le \beta_2 \le 0.60$) and γ ($0^o \le \gamma \le 60^o$) defomation parameters. In the present calculations, 171 evenly fixed points on $\beta_2 - \gamma$ plane have been taken into account for obtaining each PES.

4. RESULTS AND DISCUSSION

The reliable prediction of the g.s. BEs of nuclei not only in the stability line but also far from stability is a test for any nuclear model. In the present study, we have calculated the g.s. BEs of neutron-rich $^{83-91}$As isotopes by using the RMF model with DD-ME2 and DD-PC1 functionals. The calculated BE per nucleon (BE/A) for the considered isotopes are shown in Fig. 1 together with the results of the finite-range droplet model (FRDM) [33] and experimental data [34]. As can be seen in Fig. 1, the results of our calculations with DD-ME2 and DD-PC1 interactions are very close to the experimental BE/A values as well as the results of FRDM. Maximum deviation between our results obtained with the DD-ME2 and DD-PC1 functionals and experimental data is around 0.04 MeV which means that the maximum deviation from the experiment is about 0.48%. It should be noted that FRDM predicts the g.s. BE/A of $^{83-91}$As nuclei more precisely because the maximum deviation between the predicted BE/A of the considered nuclei with FRDM and experimental data is around 0.01 MeV. This success is aroused from the fitting of many parameters of FRDM by considering only BE of nuclei cover nuclidic chart [19]. Furthermore, non-relativistic counterparts of the RMF model such as Hartree–Fock–Bogoliubov method with Skyrme- and Gogny-type interactions, give somehow more precise results for the g.s. BE of nuclei when we consider a wide range of nuclei on the nuclidic chart [28]. However, the RMF model with modern parameters is still favorable for the investigations of sizes and deformations of nuclei [14, 17, 19].

We have obtained PECs of neutron-rich $^{83-91}$As isotopes for the investigation of the g.s. shape evolution of the considered isotopes. The obtained PECs from the RMF model with DD-ME2 and DD-PC1 functionals are shown in Fig. 2. For obtaining each PEC of nucleus of interest, quadrupole deformation parameter β_2 was kept fixed and the g.s. BE of the nucleus has been obtained. Later, the obtained lowest g.s. BE of nucleus was taken into account as a reference point. Thus, the PEC of a nucleus has been obtained as a function of β_2 starting from the $\beta_2 =$

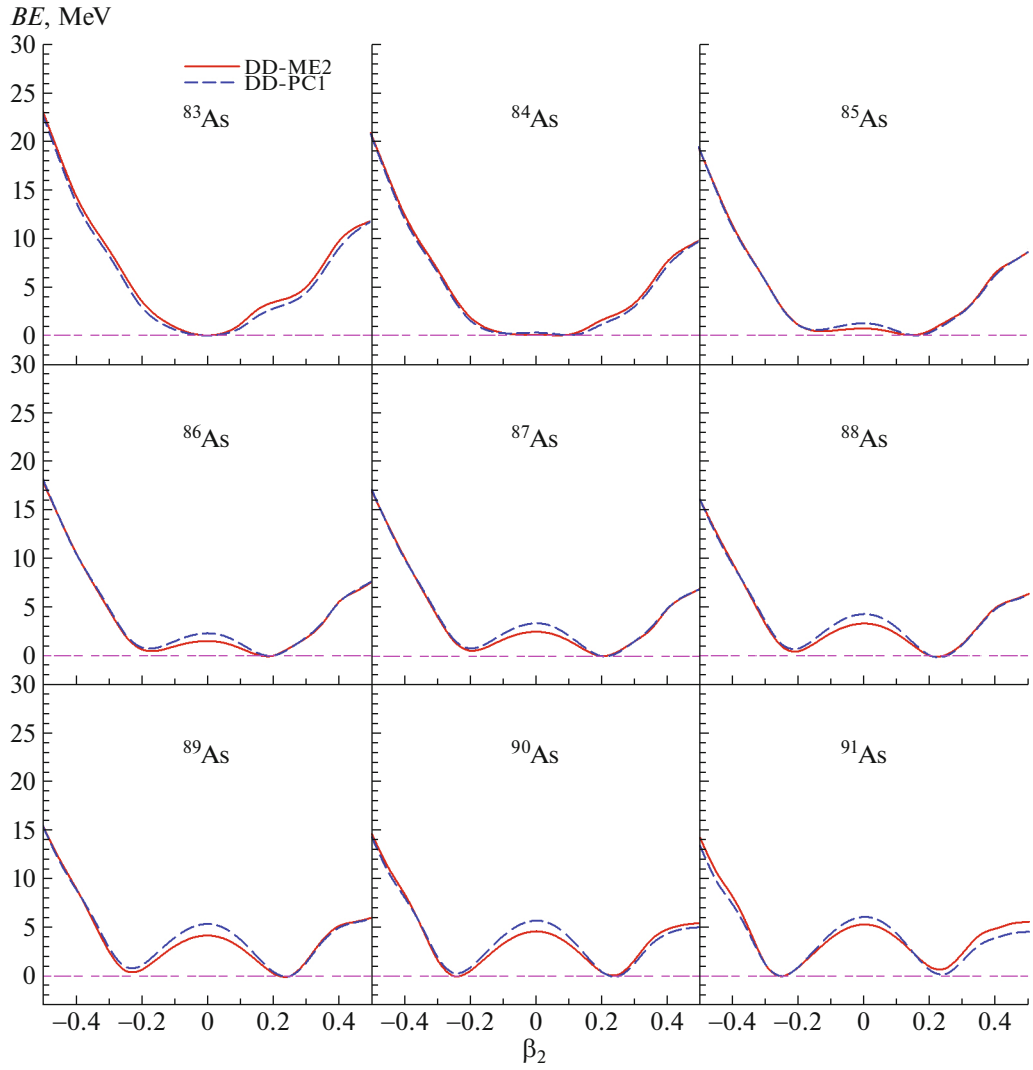


Fig. 2. The obtained PECs of $^{83-91}$As isotopes as a funtion of β_2 by using quadrupole moment constrained RMF model with DD-ME2 and DD-PC1 interactions. In these figures the BE of g.s. is taken as a reference.

-0.5 to $\beta_2 = 0.5$. As is seen in Fig. 2, both DD-ME2 and DD-PC1 interactions give similar PEC for each As nuclei. The PEC of ^{83}As has a minimum around $\beta_2 = 0$ which means that it is spherical in its g.s. As is well known, ^{83}As has proton number $Z = 33$ and neutron number $N = 50$ which is magic number. It is expected that ^{83}As should be spherical because of its neutron shell closure as suggested in our PEC reults. The PECs of ^{84}As and ^{85}As indicate soft deformed prolate shapes around $\beta_2 = 0.1$. Starting from ^{86}As to ^{88}As, the obtained PECs have two minimas at about $\beta_2 = -0.2$ (oblate) and $\beta_2 = 0.2$ (prolate) with a soft bump at $\beta_2 = 0$. These results can be considered as a sign of the shape transitional region of the As nuclei. In the PECs of ^{89}As, ^{90}As, and ^{91}As nuclei there can be seen two minima at about $\beta_2 = -0.23$ (oblate) and $\beta_2 = 0.23$ (prolate) with a clear bump at $\beta_2 = 0$. This can be related with γ-soft character of $^{89-91}$As nuclei. As we will later discuss, more evidence is needed for such a conclusion.

As is mentioned before, the PECs of $^{86-88}$As nuclei may indicate that these nuclei can be in the transitional region. The neutron single-particle spectra of these nuclei can give more details. By regarding this point, we have presented the calculated neutron single-partile levels of $^{86-88}$As nuclei in Fig. 3 as a function of β_2. These levels have been obtained by using the DD-ME2 functional. We have not presented the results of the DD-PC1 functional because similar results of DD-ME2 have been obtained. Dashed lines and solid lines in Fig. 3 indicate neutron single-particle levels and fermi energies, respectively. In agreement with the PECs results of $^{86-88}$As nuclei, soft bumps in fermi energies are aroused around between $\beta_2 = -0.2$ and $\beta_2 = 0.2$.

Potential energy surface can give more reliable

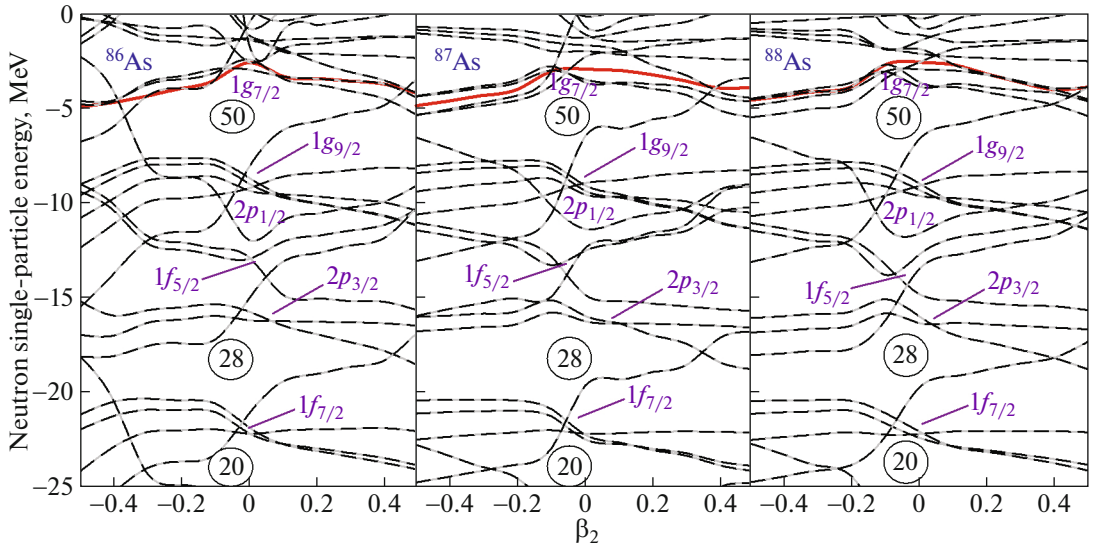


Fig. 3. The calculated neutron single-particle levels for ^{86}As, ^{87}As and ^{88}As isotopes as a function of the quadrupole deformation parameter β_2. The positions of the corresponding Fermi levels are shown by the solid line.

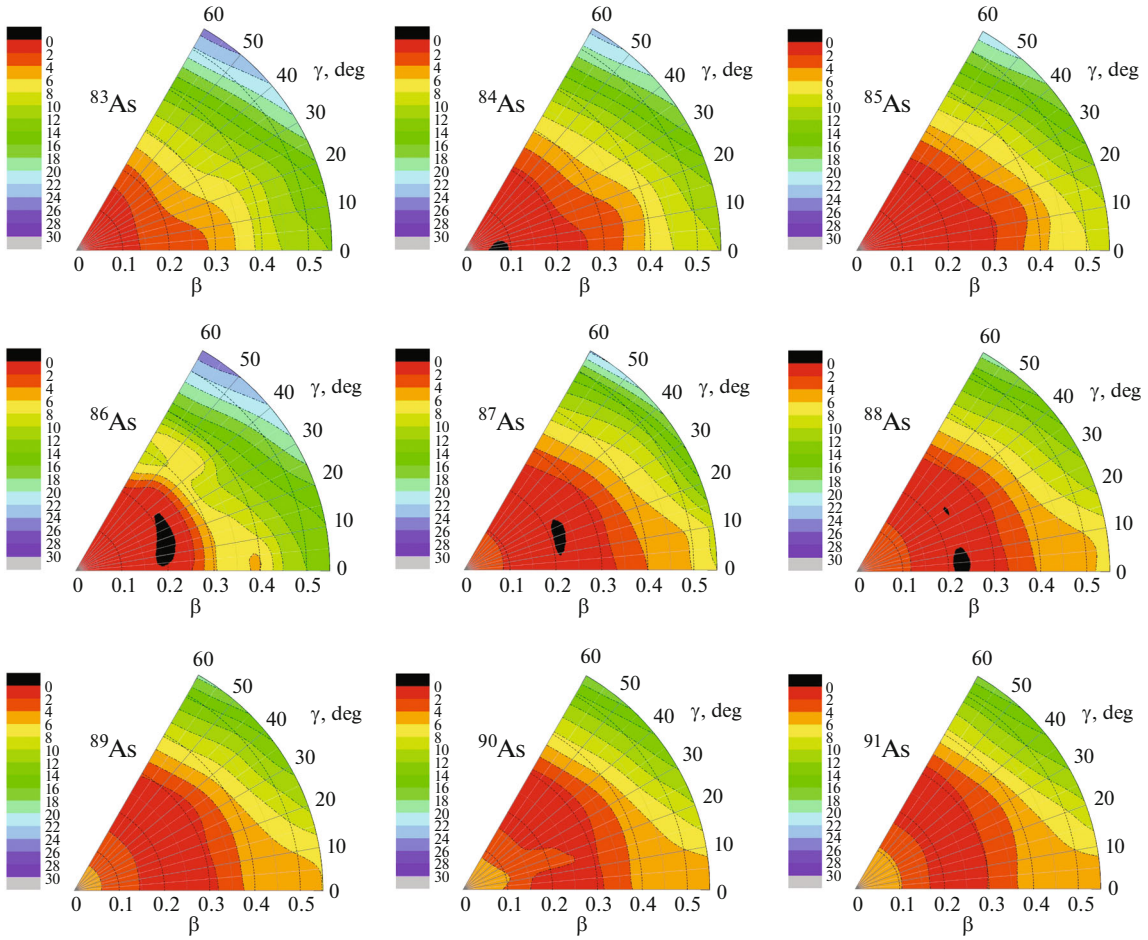


Fig. 4. The obtained PESs for $^{83-91}$As isotopes by using triaxial symmetric RMF calculations with DD-ME2 interaction. Contour lines represent a step of 2 MeV and the BE is set to zero at the minimum of each surface.

evidence for determinations of the g.s. shape evolution of an isotopic chain. In the present study, we have obtained PESs of $^{83-91}$As nuclei in the RMF model with DD-ME2 (Fig. 4) and DD-PC1 (Fig. 5) interactions. For obtaining PES for each nuclei on the $\beta_2 - \gamma$ plane, the g.s. BE of nuclei has been

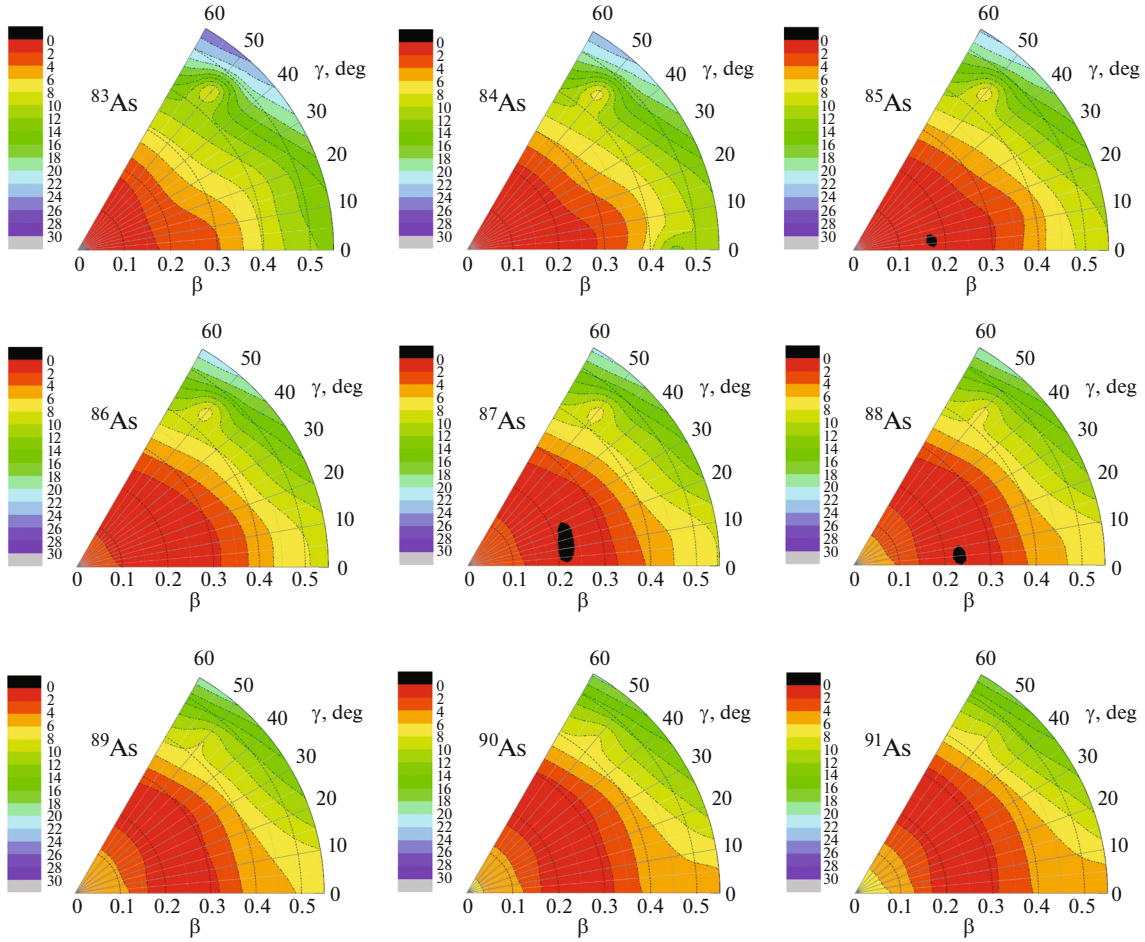


Fig. 5. The same as Fig. 4 but obtained by using DD-PC1 interaction.

calculated by keeping fixed the β_2 and γ deformation parameter values. The lowest g.s. BE of nuclei of interest has been taken as a reference point. As can be seen in Fig. 4, the g.s. shape of ^{83}As nucleus has been predicted to be spherical by DD-ME2 functional in agreement with the PEC results. Soft prolate deformed shape is predicted for the ^{84}As, while ^{85}As is seen as to be spherical. It can be said that the PESs of $^{86-88}$As may have indications as to be triaxial nuclei. The rest of PESs show that $^{89-91}$As nuclei can be possibly determined as to be γ-soft rotor in their g.s. Similar results for $^{89-91}$As nuclei can be deduced from Fig. 5 obtained with DD-PC1 functional. Differently from Fig. 4, the ^{85}As and ^{86}As are predicted to have prolate deformed shape and γ-soft rotor by DD-PC1 functional, respetively. In both Fig. 4 and Fig. 5, the PES of ^{87}As has a minimum at about $\beta_2 = 0.2$ and $\gamma = 20^o$ which means that this nucleus can be a possible candidate for being a triaxial nucleus.

Apart from the discussion on the g.s. shape evaluation of neutron-rich $^{83-91}$As isotopes, we have also obtained some nuclear g.s. properties of the considered nuclei by using the RMF model with DD-ME2 and DD-PC1 functionals. The calculated BE/A, two-neutron separation energy (S_{2n}), root-

Table 1. The calculated g.s. properties of neutron-rich $^{83-91}$As isotopes with DD-ME2 interaction (see text for details)

Nucleus	BE/A, MeV	S_{2n}, MeV	r_c, fm	β_2	Q_t, b
^{83}As	8.600	13.316	4.102	0.000	−0.006
^{84}As	8.536	3.228	4.116	0.081	1.428
^{85}As	8.481	3.908	4.138	0.156	2.786
^{86}As	8.430	4.045	4.157	0.189	3.452
^{87}As	8.379	4.010	4.174	0.211	3.920
^{88}As	8.328	3.938	4.190	0.227	4.302
^{89}As	8.277	3.748	4.205	0.239	4.614
^{90}As	8.220	3.179	4.217	0.237	4.665
^{91}As	8.162	2.911	4.388	0.233	4.675

Table 2. The same as Table 1 but obtained by using DD-PC1 interaction

Nucleus	BE/A, MeV	S_{2n}, MeV	r_c, fm	β_2	Q_t, b
^{83}As	8.639	14.615	4.112	0.000	0.000
^{84}As	8.581	3.720	4.125	0.100	1.749
^{85}As	8.531	4.336	4.141	0.148	2.667
^{86}As	8.483	4.431	4.162	0.199	3.597
^{87}As	8.434	4.165	4.171	0.192	3.610
^{88}As	8.384	4.106	4.199	0.250	4.744
^{89}As	8.336	4.066	4.207	0.245	4.634
^{90}As	8.280	3.284	4.220	0.246	4.725
^{91}As	8.222	3.061	4.233	0.252	4.941

mean-square (rms) charge radii (r_c), quadrupole deformation parameter (β_2) and total quadrupole moment (Q_t) of As isotopes by using DD-ME2 interaction are listed in Table 1 for giving more details. Also, a similar table obtained by using DD-PC1 interaction is presented in Table 2.

5. CONCLUSIONS

The RMF model with two interactions DD-ME2 and DD-PC1 has been used to investigate the g.s. properties of the neutron-rich $^{83-91}$As isotopes. The g.s. BE/A of the considered isotopic chain have been obtained in agreement with the experimental data. Also, the two-neutron separation energy, rms charge radii, (β_2) and total quadrupole moment (Q_t) of As isotopes have been obtained. By using the calculated PECs and PESs of the considered isotopic chain, ^{87}As nucleus has been suggested to be a possible candidate for triaxial nucleus.

REFERENCES

1. P. Cejnar, J. Jolie, and R. F. Casten, Rev. Mod. Phys. **82**, 2155 (2010).
2. A. Bohr and B. M. Mottelson, *Nuclear Structure*, Vol. 2 (Benjamin, New York, 1975).
3. W. Greiner and J. Maruhn, *Nuclear Models* (Springer, Berlin, 1996).
4. R. F. Casten and E. A. McCutchan, J. Phys. G: Nucl. Part. Phys. **34**, R285 (2007).
5. C. Chandler, P. H. Regan, C. J. Pearson, B. Blank, A. M. Bruce, W. N. Catford, N. Curtis, S. Czajkowski, W. Gelletly, R. Grzywacz, Z. Janas, M. Lewitowicz, C. Marchand, N. A. Orr, R. D. Page, A. Petrovici, A. T. Reed, M. G. Saint-Laurent, S. M. Vincent, R. Wadsworth, D. D. Warner, and J. S. Winfield, Phys. Rev. C **56**, R2924(R) (1997).
6. M. Bender, P. Bonche, and P.-H. Heenen, Phys. Rev. C **74**, 024312 (2006).
7. A. Obertelli, T. Baugher, D. Bazin, J. -P. Delaroche, F. Flavigny, A. Gade, M. Girod, T. Glasmacher, A. Goergen, G. F. Grinyer, W. Korten, J. Ljungvall, S. McDaniel, A. Ratkiewicz, B. Sulignano, and D. Weisshaar, Phys. Rev. C **80**, 031304(R) (2009).
8. J. A. Briz, E. Nácher, M. J. G. Borge, A. Algora, B. Rubio, Ph. Dessagne, A. Maira, D. Cano-Ott, S. Courtin, D. Escrig, L. M. Fraile, W. Gelletly, A. Jungclaus, G. Le Scornet, F. Maréchal, Ch. Miehé, et al., Phys. Rev. C **92**, 054326 (2015).
9. Z. Shi and Z. P. Li, Phys. Rev. C **97**, 034329 (2018).
10. K. Nomura, R. Rodríguez-Guzmán, and L. M. Robledo, Phys. Rev. C **95**, 064310 (2017).
11. C. M. Petrache, I. Ragnarsson, Hai-Liang Ma, R. Leguillon, T. Konstantinopoulos, T. Zerrouki, D. Bazzacco, and S. Lunardi, Phys. Rev. C **88**, 051303(R) (2013).
12. D. Vautherin and D. M. Brink, Phys. Rev. C **5**, 626 (1972).
13. J. Dechargé and D. Gogny, Phys. Rev. C **21**, 1568 (1980).
14. P. Ring, Prog. Part. Nucl. Phys. **37**, 193 (1996).
15. D. Vretenar, A. V. Afanasjev, G. A. Lalazissis, and P. Ring, Phys. Rept. **409**, 101 (2005).
16. J. Meng, H. Toki, S. G. Zhou, S. Q. Zhang, W. H. Long, and L. S. Geng, Prog. Part. Nucl. Phys. **57**, 470 (2006).
17. Y. K. Gambhir and A. Bhagwat, Phys. Part. Nucl. **37**, 194 (2006).
18. J. Piekarewicz, Phys. Rev. C **76**, 064310 (2007).
19. T. Bayram and A. H. Yilmaz, Mod. Phys. Lett. A **28**, 1350068 (2013).
20. T. Bayram, S. Akkoyun, and Ş. Şentürk, Phys. At. Nucl. **81**, 288 (2018).
21. T. Bayram and S. Akkoyun, Phys. Scripta **87**, 065201 (2013).
22. J. D. Walecka, Ann. Phys. (N. Y.) **83**, 491 (1974).
23. J. Boguta and A. R. Bodmer, Nucl. Phys. A **292**, 413 (1977).
24. Y. Sugahara and H. Toki, Nucl. Phys. A **579**, 557 (1994).
25. H. Lenske and C. Fuchs, Phys. Lett. B **345**, 355 (1995).
26. H. Shen, Y. Sugahara, and H. Toki, Phys. Rev. C **55**, 1211 (1997).
27. J. Piekarewicz, Phys. Rev. C **66**, 034305 (2002).
28. D. Peña-Arteaga, S. Goriely, and N. Chamel, Eur. Phys. J. A **52**, 320 (2016).
29. T. Nikšić, N. Paar, D. Vretenar, and P. Ring, Comput. Phys. Commun. **185**, 1808 (2014).
30. G. A. Lalazissis, T. Nikšić, D. Vretenar, and P. Ring, Phys. Rev. C **71**, 024312 (2005).
31. T. Nikšić, D. Vretenar, and P. Ring, Phys. Rev. C **78**, 034318 (2008).
32. G. A. Lalazissis, S. Karatzikos, R. Fossion, D. Pena Artega, A. V. Aanasjev, and P. Ring, Phys. Lett. B **671**, 36 (2009).
33. P. Möller, J. R. Nix, and K.-L. Kratz, At. Data. Nucl. Data Tables **66**, 131 (1997).
34. M. Wang, G. Audi, F. G. Kondev, W. J. Huang, S. Naimi, and X. Xu, Chin. Phys. C **41**, 030003 (2017).